JMSAE

Journal of Materials Science and Applied Energy

Journal home page: jmsae.snru.ac.th

The Radiation Shielding and Exposure Buildup Factor Properties of FeMnCoCrNi HEA Alloys

Kittisak Sriwongsa [a, b, *], Punsak Glumglomchit [c], Mintharach Suwannayuha [c], Teerathat Wananuraksakul [c], Parichat Singharach [c], Sunantasak Ravangvong [d], Sakchai Glumglomjit [e]

[a] *Lecturers responsible for Bachelor of Education Program in Physics, Faculty of Education, Silpakorn University, Nakhon Pathom, 73000 Thailand*

[b] *The demonstration school of Silpakorn University, Nakhon Pathom, 73000 Thailand*

[c] *Huahin Vitthayalai School, Hua – Hin, Prachuap Khiri Khan, 77110 Thailand*

[d] *Division of Science and Technology, Faculty of Science and Technology, Phetchaburi Rajabhat University, Phetchaburi, 76000 Thailand*

[e] *School of Geotechnology, Institute of Engineering, Suranaree University of Technology, Nakhon Ratchasima, 30000 Thailand*

*Corresponding Author: sriwongsa_k@silpakorn.edu

Received 20 May 2020; **Revised** 26 May 2020; **Accepted** 9 July 2020

Abstract

In this research to estimated total and partial interaction, and radiation shielding properties of HEA alloys of FeMnCoCr, FeMnCoCrNi6 and FeMnCoCrNi14. Radiation shielding effectiveness of HEA alloys were estimated by determine μ_m, Z_{eff} and N_{el} at photon energies ranging $10^{-3} – 10^{5}$ MeV using WinXCom computer software program. EBF were simulated by G–P fitting theory at energies ranging 15 keV – 15 MeV up to deep penetration 40 mfp. The results indicated that, FeMnCoCrNi14 alloy was found excellent radiation shielding. This study indicated that FeMnCoCrNi14 can be developed for radiation shielding materials.

Keywords: HEA alloys; Radiation shielding; Exposure build–up factor

Introduction

Since starting of study and design on high entropy alloys (HEAs), indexing is record and show in Web of Science (WoS) and find that HEAs is emerging layer of alloys that are lately being popularly studied [1 – 4]. The alloy materials are found using in many sectors of industrials such as in irradiation, nuclear reactors, aerospace, engineering materials, petro–chemical industries and biomedical implants [5 – 8]. In sector of photon interaction, there are many important parameters like effective electron density (N_{el}), effective atomic number (Z_{eff}) and mass attenuation coefficient (μ_m) which helping for using to explain and design for radiation protection efficiency of medium [9, 10].

μ_m values are commonly properties for medium which discuss the probability of interaction for radiations with medium. Z_{eff} values are properties for mixture or compound like atomic number of elements. These values are specific characteristics based on energy, helps to explain efficacy for shielding of medium and interprets radiations attenuation by medium. N_{el} values are another commonly properties for interaction between radiation and medium, which let average among of electrons per unit total mass for medium data. Moreover, exposure build–up factor is popularly use research for shielding medium [11 – 13].

There are many methods to determine exposure build–up factor (EBF) like G–P fitting theory, Monte Carlo theory and iterative theory. American Nuclear Society (ANS, 1991) estimate EBF using G–P fitting theory for 23 elements at energies ranging 15 keV – 15MeV up to deep penetration 40 mfp [14].

In this context, total and partial interactions of alloy were discussed. μ_m, Z_{eff} and N_{el} values were calculated and explained at energies ranging 10^{-3} – 10^{5} MeV. Lastly, EBF properties of alloys have been computed. The computation will give useful data for alloys was use in shielding medium applications.

Theories and Computation

Shielding radiation: μ_m, Z_{eff} and N_{el}

The behavior of photoelectric absorption effect (PE), incoherent (Compton) scattering (C) and pair production (PP) interaction can be discussed by photon interaction with alloys. μ_m of alloys was the probability of interaction with medium and estimated theoretically by using mixture rule and WinXCOM software program and using following by equation (1) [15];

$$\mu_m = \sum_{i=1}^{n} w_i \mu_{mi} \tag{1}$$

Here w_i and μ_{mi} are weight fraction and total mass attenuation coefficients of i^{th} in element in mixture, respectively.

The total interaction cross–section (σ_t) of alloys have been computed with helped of μ_m and estimated by equation (2) [16];

$$\sigma_t = \frac{M \mu_m}{N_A} a \tag{2}$$

Here $M = \Sigma_i A_i n_i$ is molecular weight of alloy, A_i and n_i are atomic weight of i^{th} element and molecule amount of formula units, respectively. N_A is constant value of Avogadro. Effective atomic cross–section ($\sigma_{t,a}$) were computed by equation (3) [16, 17];

$$\sigma_{t,a} = \frac{\sigma_t}{\sum_i n_i} \tag{3}$$

Total electron cross–section ($\sigma_{t,el}$) were determined by equation (4) [17, 18];

$$\sigma_{t,el} = \frac{1}{N_A}\sum_i \frac{f_i A_i}{z_i}(\mu_m)_i \tag{4}$$

Here f_i is fractional abundance of i^{th}, Z_i is atomic number of i^{th} element. Z_{eff} values have been simulated from equation (5) [16 – 18];

$$Z_{eff} = \frac{\sigma_{t,a}}{\sigma_{t,el}} \tag{5}$$

The N_{el} of alloys have been computed from equation (6);

$$N_{el} = \frac{Z_{eff} N_A}{M}\sum_i n_i \tag{6}$$

Exposure build–up factor (EBF)

EBF value is commonly value used design medium for radiation shielding. EBF was obtained by computing from Geometrical Progression (G–P) fitting method at energy ranging 15 keV – 15 MeV and this value can be following from equation (7) – (9). Firstly, the knowledge of equivalent atomic number (Z_{eq}) value is very important as Z_{eq} values must lie at specific energies between Z_1 and Z_2 atomic numbers ($Z_1 < Z_{eq} < Z_2$) [19, 20].

$$B(E,x) = 1 + \frac{b-1}{K-1}(K^x - 1), K \neq 1 \tag{7}$$

$$B(E,x) = 1 + (b-1)x, K = 1 \tag{8}$$

Here E and K are energy and multiplication factor per mfp, respectively and K was obtained from equation (9);

$$K(E,x) = cx^{\mathrm{a}} + d\,\frac{\tanh\tanh\left(\dfrac{x}{x_k} - 2\right) - \tanh(-2)}{1 - \tanh(-2)}, x \leq 40\text{mfp} \tag{9}$$

Here x is distance traveled in mfp. b is buildup factor at 1 mfp. X_k, a, b, c and d are parameters of G–P fitting.

Results and Discussion

The compositions for FeMnCoCrNi HEA alloys are presented in Table 1. The total and partial interaction, μ_m, Z_{eff} and N_{el} at energies ranging 10^{-3} – 10^5 MeV for alloy samples have been shown in Fig. 1 – 4, respectively. The EBF values of alloys with energies at different deep penetration (1, 5, 10, 15, 20, 25, 30, 35, and 40 mfp) are presented in Fig. 6 (a) – (c). The EBF values for alloys with deep penetrations at energy 0.015, 0.15, 1.50, and 15 MeV are presented in Fig. 7 (a) – (d).

Table 1 Composition of FeMnCoCrNi alloys.

Sample	Weight fraction				
	Fe	**Mn**	**Co**	**Cr**	**Ni**
FeMnCoCr	0.50	0.30	0.10	0.10	–
FeMnCoCrNi6	0.34	0.20	0.20	0.20	0.06
FeMnCoCrNi14	0.20	0.20	0.20	0.26	0.14

The total and partial interaction and μ_m of alloys

The μ_m of total and partial photon interaction was exhibited in Fig. 1; results from FeMnCoCrNi14, at different photon energy ranging, there are three partial interaction processes: 1. photoelectric absorption effect (PE) at low energy (1 – 500 keV), 2. incoherent (Compton) scattering (C) at intermediate energy (500 keV – 1 MeV) and 3. pair production (PP) at high energy (1 MeV – 100 GeV). From Fig. 1, for energies more than 10 keV and 50 keV, μ_m of coherent and incoherent (Compton) scattering was decreased sharply, respectively, that due to both are inverse with photon energies. The change of μ_m for C occurred chemical composite whereas it had μ_m trend like coherent scattering. The μ_m of PE was decreased rapidly with increased photon energies that may be due to occurred from the change in cross section of photoelectric by inversely proportional of photon energies $E^{3.5}$. The chemical compositions of alloy are important due to μ_m for PE dependence on atomic number of medium by interaction is Z^{4-5}. The μ_m of PP in nuclear field and electric field was increased to 500 MeV and therefore it nearly constant that due to μ_m of PP was direct variation with log E. The PP in nuclear field and electric field were dependence on Z^2 and nearly linear constant, respectively.

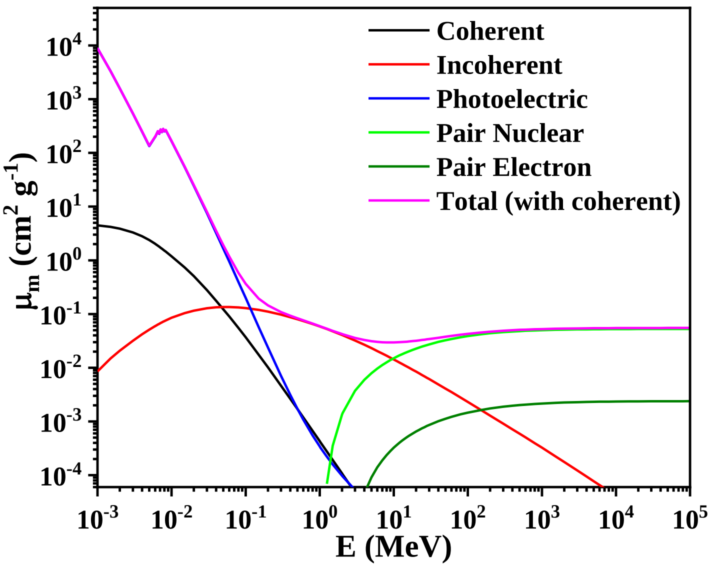

Fig. 1 Interaction of FeMnCoCrNi14 alloy at energies ranging 10^{-3} – 10^5 MeV for total and partial (with coherent).

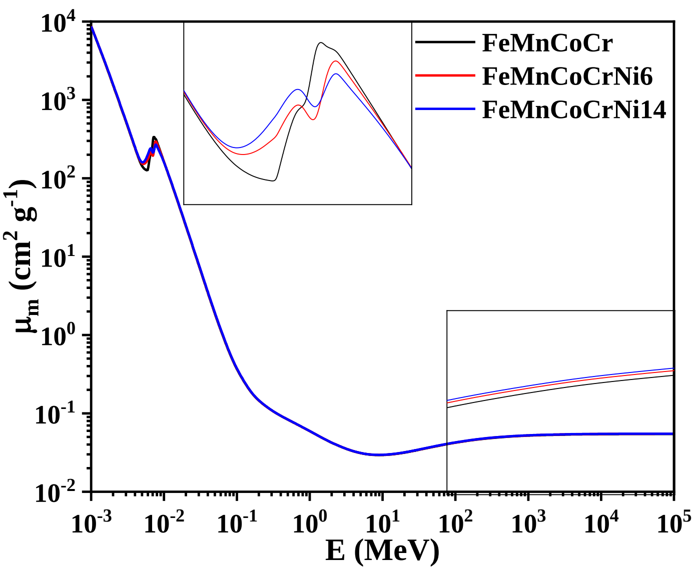

Fig. 2 μ_m of alloy samples at energies ranging 10^{-3} – 10^5 MeV.

The μ_m values of alloy samples in this work were calculated from WinXCom software program at energy ranging 10^{-3} – 10^5 MeV. Figure 2 is presented μ_m values of all alloy samples which decrease exponentially with increasing energies. It is noted that μ_m values of alloy samples are very high at low energy ranging and decrease quickly with increasing energies. Intermediate energies ranging, μ_m values decrease, while at high energy ranging μ_m values constant with increasing energies. These results can be discussed on photon interaction with medium. The PE and PP will appear at lower and higher energy ranging while at intermediate energy ranging the C is major one. At low energy ranging, curve is not continuous that because of absorption edge of elements as exhibited in Table 2. It is clear that μ_m value increase with increasing Ni content in alloys. This increasing because of replacement of Fe (Z = 26) with Ni (Z = 28) and μ_m value of FeMnCoCrNi14 is the highest among alloys, so, FeMnCoCrNi14 is excellent radiation shielding alloy.

Table 2 absorption edge of elements (keV).

Edge	Elements				
	Cr	**Mn**	**Fe**	**Co**	**Ni**
K	5.99	6.54	7.11	7.71	8.33
L1	–	–	–	–	1.01

Z_{eff} and N_{el} of alloys

The Z_{eff} and N_{el} values with energies for all alloy samples have been presented in Fig. 3 and Fig. 4, respectively. From Fig. 3, Z_{eff} value, for all alloy samples, increases with increasing of energies until 5 keV and suddenly drops at 5 – 6 keV. These suddenly drops can be discussed by atomic number of Cr (Z = 24) as 24.98 for FeMnCoCr, 24.83 for FeMnCoCrNi6 and 24.76 for FeMnCoCrNi14 [21]. In addition, the maximum Z_{eff} value was found for FeMnCoCrNi14 alloy. This can be discussed on fundamental of weight fraction which FeMnCoCrNi14 has Ni content highest. The N_{el} value of alloys has shown the same trend and behavior similar Z_{eff} value as presented in Fig. 4.

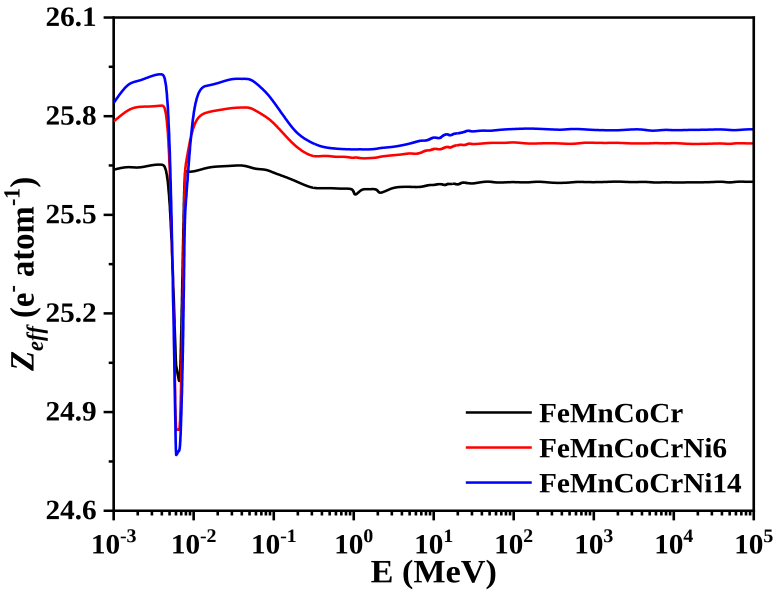

Fig. 3 Z_{eff} of alloy samples at photon energy ranging $10^{-3} – 10^{5}$ MeV.

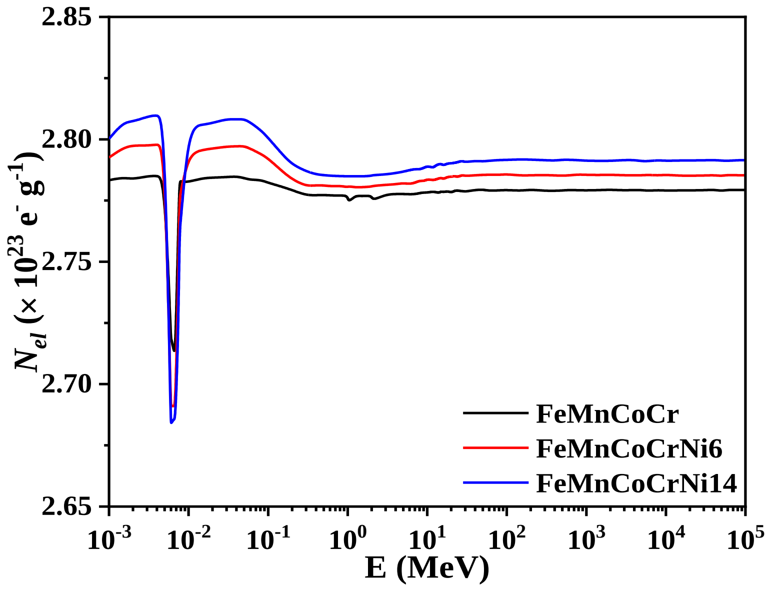

Fig. 4 N_{el} of alloy samples at photon energy ranging $10^{-3} – 10^{5}$ MeV.

EBF with photon energy

The EBF of alloy samples, at energies ranging 15 keV – 15 MeV and at different deep penetrations, has been exhibited in Fig. 6 (a) – (c). Form figures, they are observed that EBF values of all alloy samples increase until highest value at intermediate energies and then decreased. These events were discussed on fundamental of the main partial of photon interaction processes at variation energy ranging as mentioned before. At low and high energy ranging, PE and PP were main interaction process, photon will be absorbed maximum. So, EBF values are decreased. At intermediate energy ranging, C is main interaction process as EBF values increased. This interaction, photon multiples scattering which resulting in more lift time of photon is long and more probability to photon to escape medium. In fact, the increasing of deep penetration for medium that results in increase thickness, and that made photon increasing scattering in interacting medium. Especially, for medium with the highest Z_{eq} as exhibited in Fig. 5, it results in high EBF values.

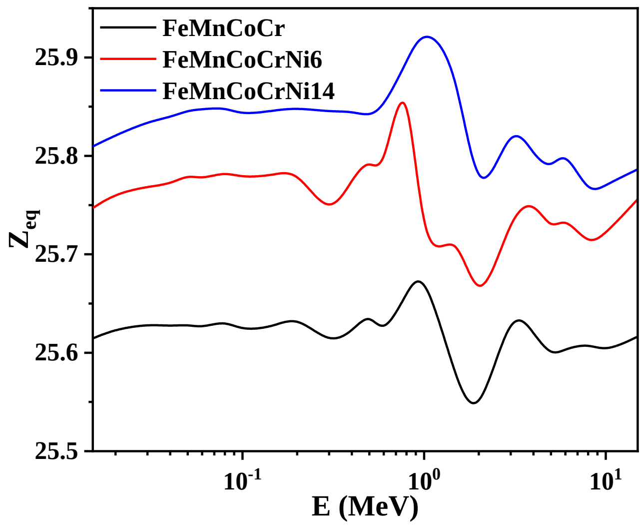

Fig. 5 Z_{eq} of alloy samples at photon energy ranging 15 keV – 15 MeV.

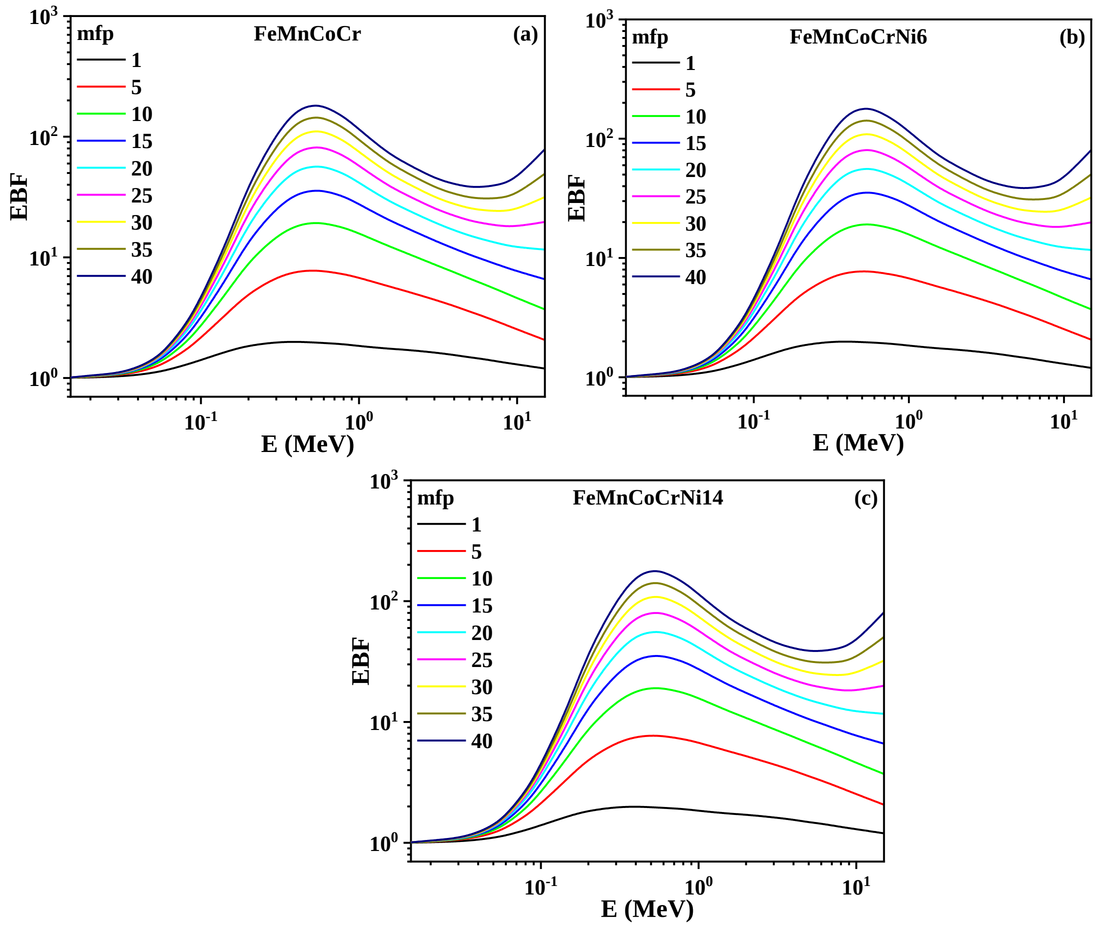

Fig. 6 EBF of (a) FeMnCoCr, (b) FeMnCoCrNi6 and (c) FeMnCoCrNi14 alloys at energies ranging 15 keV–15 MeV.

EBF with deep penetration

Figure 7 exhibit an increase values of EBF with different deep penetration and energy (0.015, 0.15, 1.50, and 15 MeV) for all alloys. These because of EBF values saturate in lager deep penetration. At 0.015 MeV, Fig. 7 (a), EBF values are nearly constant (0.0042 – 0.0117) for deep penetration, 1 – 40 mfp. From Fig. 7 (a) – (c), FeMnCoCr alloy had found maximum EBF values at energy ranging 0.015 – 0.15 MeV until 40 mfp. At energy 15 MeV, FeMnCoCrNi14 showed highest EBF that due to pair/triplet interaction of all alloys produced electron/positron pair. The rest of positrons were annihilated by electron and generate two secondary photons at energy 0.511 MeV. Photons probability for escape through higher thickness of alloys were increased, resulting in larger EBF values. Finally, the excellent radiation shielding medium, low values of buildup factors were desired.

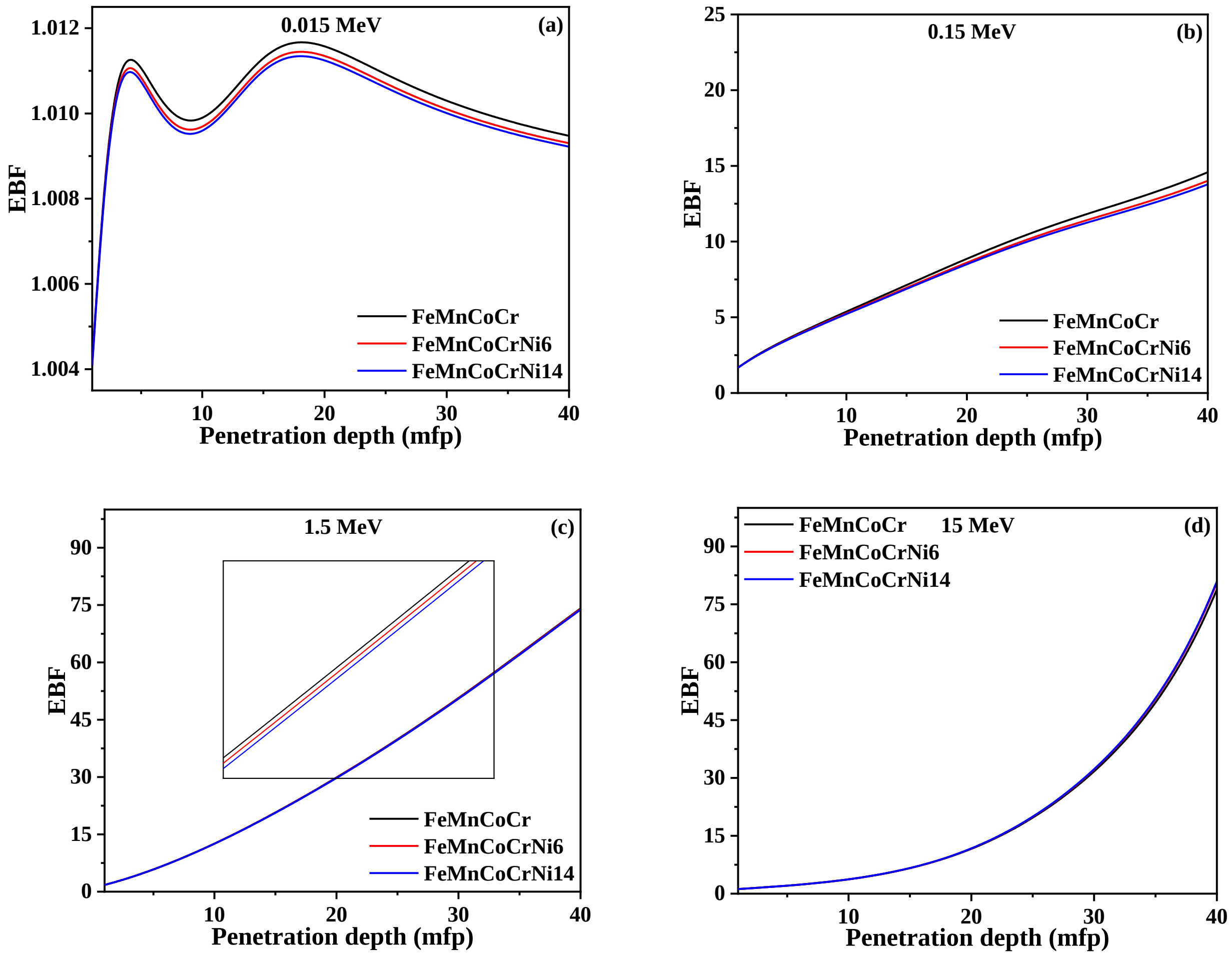

Fig. 7 EBF VS deep penetration at energies, (a) 0.015, (b) 0.15, (c) 1.5, and (d) 15 MeV.

Conclusion

The mass attenuation coefficient for total and partial photon interactions (with coherent) of alloys have been estimated at energies ranging 10^{-3} – 10^{5} MeV. The results shown that, these parameters increased with increased Ni content. At different energy ranging, at low energies, photoelectric absorption effect is major process, at intermediate energies, Compton (incoherent) scattering is main interaction process and pair production becomes main for high energies. For excellent radiation shielding medium, high value of μ_m, Z_{eff} and N_{el} are desired while buildup factors are not. The μ_m, Z_{eff} and N_{el} values in the estimated alloy systems increased as Ni content increased while EBF values decreased. Clearly, the higher of Ni content in alloys will improve radiation shielding properties. So FeMnCoCrNi14 is the excellent radiation shielding alloy because of μ_m, Z_{eff} and N_{el} values were high and EBF values were low compared with the other alloys.

Acknowledgement

This research has been supported by Research and Researcher for Industry (RRI), Thailand Research Fund (TRF) contract number. PHD59I0007.

References

[1] Y. Qiu, S. Thomas, D. Fabijanic, A.J. Barlow, H.L. Fraser, N. Birbilis, Microstructural evolution, electrochemical and corrosion properties of $Al_xCoCrFeNiTi_y$ high entropy alloys, Mater. Des. 170 (2019) 107698.

[2] F. Alijani, M. Reihanian, K. Gheisari, Study on phase formation in magnetic FeCoNiMnV high entropy alloy produced by mechanical alloying, J. Alloys. Compd. 773 (2019) 623 – 630.

[3] L.B. Chen, R. Wei, K. Tang, J. Zhang, F. Jiang, J. Sun, Ductile-brittle transition of carbon alloyed $Fe_{40}Mn_{40}Co_{10}Cr_{10}$ high entropy alloys, Mater. Lett. 236 (2019) 416 – 419.

[4] H. Jiang, L. Jiang, D. Qiao, Y. Lu, T. Wang, Z. Cao, T. Li, Effect of Niobium on Microstructure and Properties of the $CoCrFeNb_xNi$ High Entropy Alloys, J. Mater. Sci. Technol. 33 (2017) 712 – 717.

[5] B. Vishwana, K. Vaibhav, S.K. Jha, K.V. Mirji, I. Samajdar, D. Srivastava, R. Tewari, N. Saibaba, G.K. Dey, Development of Nb–1%Zr–0.1%C alloy as structural components for high temperature reactors, J. Nucl. Mater. 427 (2012) 350 – 358.

[6] X. Li, Z. Cheng, K. Hu, H. Chen, C. Yang, Crystallization kinetics and spark plasma sintering of amorphous $Ni_{53}Nb_{20}Ti_{10}Zr_8Co_6Ta_3$ powders prepared by mechanical alloying, Vacuum. 114 (2015) 93 – 100.

[7] V.P. Singh, N.M. Badiger, Gamma ray and neutron shielding properties of some alloy materials, Ann. Nucl. Energy. 64 (2014) 301 – 310.

[8] W. Jin, G. Wu, P. Li, P.K. Chu, Improved corrosion resistance of Mg–Y–RE alloy coated with niobium nitride, Thin Solid Films. 572 (2014) 85 – 90.

[9] S. Ruengsri, S. Insiripong, N. Sangwaranatee, J. Kaewkhao, Development of barium borosilicate glasses for radiation shielding materials using rice husk ash as a silica source, Prog. Nucl. Energy. 83 (2015) 99 – 104.

[10] A.M.A. Mostafa, S.A.M. Issa, M.I. Sayyed, Gamma ray shielding properties of $PbO–B_2O_3–P_2O_5$ doped with WO_3, J. Alloys. Compd. 708 (2017) 294 – 300.

[11] H. Singh, J. Sharma, T. Singh, Extensive investigations of photon interaction properties for Zn_xTe_{100-x} alloys, Nucl. Eng. Technol. 50 (2018) 1364 – 1371.

[12] S. Kaur, K.J. Singh, Investigation of lead borate glasses doped with aluminium oxide as gamma ray shielding materials, Ann. Nucl. Energy. 63 (2014) 350 – 354.

[13] M.G. Dong, X.X. Xue, Y. Elmahroug, M.I. Sayyed, M.H.M. Zaid, Investigation of shielding parameters of some boron containing resources for gamma ray and fast neutron, Results. Phys. 13 (2019) 102 – 129.

[14] M.I. Sayyed, H. Elhouichet, Variation of energy absorption and exposure buildup factors with incident photon energy and penetration depth for boro–tellurite (B_2O_3–TeO_2) glasses, Radiat. Phys. Chem. 130 (2017) 335 – 342.

[15] M.I. Sayyed, Y. Elmahroug, B.O. Elbashir, S.A.M. Issa, Gamma–ray shielding properties of zinc oxide soda lime silica glasses, J. Mater. Sci.: Mater. Electron. 28 (2017) 4064 – 4074.

[16] S.A.M. Issa, M.I. Sayyed, M.H.M. Zaid, K.A. Matori, A Comprehensive Study on Gamma Rays and Fast Neutron Sensing Properties of GAGOC and CMO Scintillators for Shielding Radiation Applications, J. Spectro. 2017 (2017) 1 – 9.

[17] N. Chanthima, J. Kaewkhao, P. Limkitjaroenporn, S. Tuscharoen, S. Kothan, M. Tungjai, S. Kaewjaeng, S. Sarachai, P. Limsuwan, Development of BaO–ZnO–B_2O_3 glasses as a radiation shielding material, Radiat. Phys. Chem. 137 (2017) 72 – 77.

[18] M.G. Dong, O. Agar, H.O. Tekin, O. Kilicoglu, K.M. Kaky, M.I. Sayyed, A comparative study on gamma photon shielding features of various germanate glass systems, Compos. Part B-Eng. 165 (2019) 636 – 647.

[19] O. Agar, E. Kavaz, E.E. Altunsoy, O. Kilicoglu, H.O. Tekin, M.I. Sayyed, T.T. Erguzel, N. Tarhan, Er_2O_3 effects on photon and neutron shielding properties of TeO_2–Li_2O–ZnO–Nb_2O_5 glass system, Results. Phys. 13 (2019) 102277.

[20] B. Oto, N. Yıldız, T. Korkut, E. Kavaz, Neutron shielding qualities and gamma ray buildup factors of concretes containing limonite ore, Nucl Eng Des. 293 (2015) 166 – 175.

[21] C. Khobkham, P. Limkitjaroenporn, K. Shimada, J. Kaewkhao, W. Chaiphaksa. Photon interaction behavior of zirconium alloy materials, Mater. Today: Proc. 5 (2018) 14928 – 14932.